Journal Article

Towards polariton blockade of confined exciton–polaritons

Author(s):
Delteil, Aymeric; Fink, Thomas; Schade, Anne; Höfling, Sven; Schneider, Christian; Imamoglu, Atac

ETH Library

Towards polariton blockade of confined exciton–polaritons

Aymeric Delteil[1*], Thomas Fink[1*], Anne Schade[2], Sven
Höfling[2,3], Christian Schneider[2] and Ataç İmamoğlu[1]

[1] *Institute of Quantum Electronics, ETH Zurich, 8093 Zurich, Switzerland.*

[2] *Technische Physik, Universität Würzburg, Würzburg, Germany.*

[3] *SUPA, School of Physics and Astronomy,*
University of St Andrews, St Andrews, UK.

[*] *These authors contributed equally to this work.*

Cavity-polaritons in semiconductor microstructures have emerged as a promising system for exploring nonequilibrium dynamics of many-body systems [1]. Key advances in this field, including the observation of polariton condensation [2], superfluidity [3], realization of topological photonic bands [4], and dissipative phase transitions [5–7], generically allow for a description based on a mean-field Gross-Pitaevskii formalism. While observation of polariton intensity squeezing [8, 30] and decoherence of a polarization entangled photon pair by a polariton condensate [10] provide counterexamples, quantum effects in these experiments show up at high polariton occupancy. Going beyond into the regime of strongly correlated polaritons requires the observation of a photon blockade effect [11, 12] where interactions are strong enough to suppress double occupancy of a photonic lattice site. Here, we report evidence of quantum correlations between polaritons spatially confined in a fibre cavity. Photon correlation measurements show that careful tuning of the coupled system can lead to a modest reduction of simultaneous two-polariton generation probability by 5 %. Concurrently, our experiments allow us to measure the polariton interaction strength, thereby resolving the controversy stemming from recent experimental reports [13]. Our findings constitute an essential step towards the realization of strongly interacting photonic systems.

Photon blockade can be described as strong conditional modification of optical properties of a medium by a single photonic excitation. The early demonstrations of photon blockade were based on the realization of the Jaynes-Cummings model consisting of a single anharmonic quantum

emitter strongly coupled to a cavity mode [14–17]. The requisite optical nonlinearity in this case originates from the impossibility of double excitation of the anharmonic emitter and consequently of the cavity-emitter system under resonant excitation. In the opposite limit of a collective excitation of a large number of two-level emitters coupled to a cavity mode, photon blockade can only be observed if there is strong interaction between optically excited collective states. This for example is manifestly the case if the incident field creates a collective excitation to a Rydberg state with large van der Waals interactions [18, 19]. In condensed matter, an analogous situation can be obtained using quantum well (QW) excitons nonperturbatively coupled to a cavity mode, leading to the formation of hybrid light-matter eigenstates, termed polaritons. In this system, exciton-exciton interactions ensure that the polariton spectrum is anharmonic, provided that polaritons are confined to maximize their in-plane spatial overlap. If the interaction-induced energy shift is larger than the polariton linewidth, the system exhibits polariton blockade [12]. A convenient verification of the blockade phenomenon is provided by photon antibunching – a vanishing photon correlation function $g^{(2)}(\tau)$ for delays τ smaller than the polariton lifetime. Even in the limit where the nonlinearity is smaller than the linewidth, finite photon antibunching can be observed provided that the laser is detuned from the polariton centre frequency. Such an observation confirms a first-order modification of the cavity transmission conditioned on the excitation of a single polariton [20].

To demonstrate quantum correlations of confined polaritons, we measure $g^{(2)}(\tau)$ using photons transmitted from a resonantly driven zero-dimensional cavity that is strongly coupled to the excitonic transition of a QW [7, 21]. Figure 1a depicts the experimental set-up based on a semi-integrated fibre cavity whose length is tunable *in situ* using a piezo-based nanopositioner. The concave surface of the fibre leads to lateral confinement with a mode waist of $w_0 = 1.0$ μm. A single InGaAs QW is placed at an antinode of the fundamental TEM_{00} mode (see Methods). When scanning the cavity mode energy across the exciton resonance, we observe a large Rabi splitting of $E_\mathrm{R} = 3.5$ meV between the two polariton eigenmodes, signaling the strong coupling regime (Fig. 1b). Focusing exclusively on the lower polariton (LP) mode and neglecting the role of the far detuned upper polariton branch, the Hamiltonian describing the system in the rotating basis under resonant drive reads:

$$H = (\hbar\omega_\mathrm{L} - E_\mathrm{LP})\hat{p}^\dagger\hat{p} + \frac{U_\mathrm{pp}}{2}\hat{p}^\dagger\hat{p}^\dagger\hat{p}\hat{p} + \hbar F^*\hat{p}^\dagger + \hbar F\hat{p} \tag{1}$$

where $\hat{p}$ denotes the lower polariton annihilation operator, ω_L the excitation laser frequency, E_LP

the LP energy, F the drive strength, and U_{pp} the polariton-polariton interaction strength. The polariton annihilation operator $\hat{p}$ can be decomposed into its exciton and photon components as $\hat{p} = c_{\mathrm{p}}\hat{a} + c_{\mathrm{x}}\hat{x}$, where $\hat{a}$ ($\hat{x}$) denotes the annihilation operator associated with the cavity mode (QW exciton). The corresponding Hopfield coefficients c_{p} and c_{x}, satisfying $|c_{\mathrm{p}}|^2 + |c_{\mathrm{x}}|^2 = 1$, depend on the cavity-exciton detuning and therefore can be adjusted by changing the cavity length.

In the limit of a small nonlinearity, the maximum degree of antibunching $A \triangleq \max\left(1 - g^2(0)\right)$ is approximately given by the ratio between the polariton-polariton interaction energy and the linewidth Γ_{p}: $A \approx U_{\mathrm{pp}}/\Gamma_{\mathrm{p}} = U_{\mathrm{xx}}|c_{\mathrm{x}}|^4/\Gamma_{\mathrm{p}}$ where U_{xx} is the exciton-exciton interaction energy (see Supplementary Information). Thus, the maximum antibunching is the result of an interplay between polariton linewidth and exciton content. In the following we identify the optimal system parameters allowing the observation of antibunching by characterizing the dependence of the lower polariton linewidth and maximum transmission on the cavity mode energy. We perform laser scans of the transmission while varying the cavity length (Fig. 2a), from which we extract the linewidth and maximum transmission. Figure 2b plots the cavity linewidth and transmission as a function of the LP energy: as we increase E_{LP} by reducing the cavity length, the linewidth experiences a moderate increase up to $E_{\mathrm{LP}} \approx 1.468$ eV. For higher E_{LP}, the linewidth increases sharply while the corresponding maximum transmission drops.

In order to identify the contributions to the polariton linewidth, we model the optical response of our cavity with an input-output formalism [22] where we use experimentally measured parameters: the Rabi splitting $E_{\mathrm{R}} = 3.5$ meV, the disorder dominated (bare) exciton linewidth $h\Delta\nu_{\mathrm{x}} = 0.5$ meV measured outside the cavity, and the bare cavity linewidth $\kappa = 28$ μeV. The only free parameter in our model is a Markovian exciton decay rate γ_{x}. We obtain the best agreement with experimental data for $\gamma_{\mathrm{x}} = 40$ μeV (see Supplementary Information). Although the physical process associated with γ_{x} is unclear, we tentatively attribute this decay channel to disorder mediated coupling of the confined LP mode to guided modes of the planar structure. A better understanding of this decay channel would be beneficial since its elimination could lead to a sizable increase in the degree of antibunching. On the other hand, the coupling to localized exciton states has only little effect on the polariton linewidth as long as we maintain negligible overlap between the LP mode and the inhomogeneously broadened bare exciton spectrum [23].

This characterization allows to identify the optimal cavity-exciton detuning $\delta_{\mathrm{c-x}}$ for maximizing quantum correlations between polaritons, or equivalently, $A \propto |c_{\mathrm{x}}|^4/\Gamma_{\mathrm{p}}$. Figure 2c shows this ratio

calculated for both our data and our model, as a function of the exciton content. We deduce from this plot that the exciton content at which we expect the highest degree of antibunching is about $|c_x|^2 \sim 0.6$, yielding a polariton lifetime of $\tau_{LP} = \hbar/\Gamma_p \approx 11$ ps. In the following we use the corresponding optimal value of δ_{c-x}.

Since τ_{LP} is shorter than the time resolution of single-photon detectors, we employ a pulsed excitation where the pulse width τ_L of the laser pulses is a factor of ≈ 3 longer than τ_{LP} [24]. The only requirement on detector bandwidth in this case is that it exceeds the laser repetition rate of 80 MHz. This approach allows us to implement a red-detuned excitation where all laser frequency components satisfy $\hbar\omega_L < E_{LP}$, thereby ensuring that A is maximal for repulsive interactions ($U_{pp} > 0$). On the other hand, we cannot rule out multiple excitations during the timescale given by τ_L, which reduces the magnitude of the measured A.

Photons emitted from the cavity are collected in a single mode fibre and transferred to a Hanbury Brown and Twiss setup where the coincidences are recorded. The upper (lower) panel of Fig. 3a shows the histogram obtained at $\Delta = \hbar\omega_{L0} - E_{LP} = -0.75\Gamma_p$ ($+0.5\Gamma_p$), where ω_{L0} denotes the centre frequency of the laser pulse. In the red-detuned case ($\Delta < 0$), we observe that the number of coincidences corresponding to a period difference of 0 is lower than the average value of the other periods, while the opposite is true for the blue-detuned case. We deduce from each histogram the corresponding integrated second order correlation $\tilde{g}^2[0]$ (see Methods).

Figure 3b shows $\tilde{g}^2[0]$ as a function of the laser detuning, obtained by repeating such measurements while scanning the laser energy. We observe a minimum of $\tilde{g}^2[0] = 0.95 \pm 0.02$ for $\Delta = -0.75\Gamma_p$. The values for $\Delta = 0$ and $\Delta < -\Gamma_p$ lie above unity; we tentatively attribute this bunching signal, not captured by the simple single mode Kerr Hamiltonian, to feeding of the LP resonance by a thermal localized exciton bath. Repeating these measurement for higher incident laser powers allows us to obtain the data shown in Fig. 3c. We used power- and detuning-dependent integration times, varying from 0.5 h to 8.5 h per point, for a total measurement time of 82 h. It is evident that photon antibunching is present for small red detunings and incident laser power not exceeding 20 nW. The lowest point at $P = 10$ nW is more than 3 sigma away from the classical limit, corresponding to a probability lower than 10^{-3} than the measured statistics originate from classical light.

The determination of U_{xx} has been previously carried out using the polariton density dependent blue shift of the LP resonance. Such measurements, however, are inherently inaccurate due to

the difficulty in estimating the actual exciton population which has contributions not only from polaritons but also from long-lived localized excitons. The latter are generated even under resonant excitation, as evidenced by the bunching signal we observe for $\Delta = 0$. On the other hand, the minimum value of $\tilde{g}^{(2)}$ directly gives a lower bound on U_{xx} without requiring an estimation of the exciton population (see Supplementary Material). From our measurements we estimate $U_{pp} = 13 \pm 6$ μeV, yielding $U_{xx} = 40 \pm 20$ μeVμm^2, in agreement with what has been estimated by several groups [6, 24–26].

Our results demonstrate that the cavity-exciton response to a drive field can be sizably modified by the prior detection of a single polariton. Together with Ref. [24], our observations demonstrate quantum behavior of polaritons that cannot be captured by mean-field methods. While the degree of quantum correlations we report are modest, further enhancement of the degree of antibunching could be reached by decreasing the polariton linewidth by employing higher quality QW samples with reduced disorder. Reducing the exciton pure dephasing using a gated structure would ensure polariton linewidths smaller than that of the bare cavity mode (see Supplementary Information), which should in turn increase the ratio U_{pp}/Γ by a factor 4. Alternatively, U_{xx} could be enhanced at least by a factor 5 by using dipolar polaritons in coupled QWs [27] or in polarized large QWs [28] embedded in microcavities, or polaron-polaritons in the fractional quantum Hall regime [29]. Finally, increasing the optical confinement using photonic microstructures [30] would also help reaching the regime of strongly interacting polaritons.

---

[1] Carusotto, I. & Ciuti, C. Quantum fluids of light. *Rev. Mod. Phys.* **85**, 299 (2013).

[2] Kasprzak *et al.* Bose-Einstein condensation of exciton polaritons. *Nature* **443**, 409-414 (2006).

[3] Amo, A. *et al.* Superfluidity of polaritons in semiconductor microcavities. *Nat. Phys.* **5**, 805-808 (2009).

[4] Lasing in topological edge states of a one-dimensional lattice. *Nat. Photon.* **11**, 651-656 (2017).

[5] Ohadi, H. *et al.* Spin order and phase transitions in chains of polariton condensates. *Phys. Rev. Lett.* **119**, 067401 (2017).

[6] Rodriguez, S.R.K. *et al.* Probing a dissipative phase transition via dynamical optical hysteresis. *Phys. Rev. Lett.* **118**, 247402 (2017).

[7] Fink, T., Schade, A., Höfling, S., Schneider, C. & Imamoğlu, A. Signatures of a dissipative phase transition in photon correlation measurements. Nat. Phys. **14**, 365-369 (2018).

[8] Karr, J. Ph., Baas, A., Houdre, R. & Giacobino, E. Squeezing in semiconductor microcavities in the

strong coupling regime. *Phys. Rev. A* **69**, 031802(R) (2004).

[9] Boulier, T., Bamba, M., Amo, A., Adrados, C., Lemaître, A., Galopin, E., Sagnes, I., Bloch, J., Ciuti, C., Giacobino, E. & Bramati, A. Polariton-generated intensity squeezing in semiconductor micropillars. *Nat. Commun.* **5**, 3260 (2014).

[10] Cuevas, A. *et al.* First observation of the quantized exciton-polariton field and effect of interactions on a single polariton. Sci. Adv. **4**, eaao6814 (2018).

[11] Imamoğlu, A., Schmidt, H., Woods, G. & Deutsch, M. Phys. Rev. Lett. Strongly interacting photons in a nonlinear cavity. *Phys. Rev. Lett.* **79**, 1467 (1997).

[12] Verger, A., Ciuti, C. & Carusotto, I. Polariton quantum blockade in a photonic dot. *Phys. Rev. B* **73**, 193306 (2006).

[13] Sun, Y. *et al.* Direct measurement of polariton-polariton interaction strength. *Nat. Phys.* **13**, 870-875 (2017).

[14] Birnbaum, K. M., Boca, A., Miller, R., Boozer, A. D., Northup, T. E. & Kimble, H. J. Photon blockade in an optical cavity with one trapped atom. Nature **436**, 87-90 (2005).

[15] Faraon, A., Fushman, I., Englund, D., Stoltz, N., Petroff, P. & Vučković, J. Coherent generation of non-classical light on a chip via photon-induced tunnelling and blockade. Nature Phys. **4**, 859-863 (2008).

[16] Lang, C. *et al.* Observation of resonant photon blockade at microwave frequencies using correlation function measurements. Phys. Rev. Lett. **106**, 243601 (2011)

[17] Reinhart, A. *et al.* Strongly correlated photons on a chip. Nature Photon. textbf6, (2012).

[18] Cubel Liebisch, T., Reinhard, A., Berman, P. R. & Raithel, G. Atom Counting Statistics in Ensembles of Interacting Rydberg Atoms. *Phys. Rev. Lett.* **95**, 253002 (2005).

[19] Urban, E. *et al.* Observation of Rydberg blockade between two atoms. *Nat. Phys.* **5**, 110-114 (2009).

[20] Ferretti *et al.* Single-photon nonlinear optics with Kerr-type nanostructured materials. *Phys. Rev. B* **85**, 033303 (2012).

[21] Besga, B. *et al.* Polariton boxes in a tunable fibre cavity. *Phys. Rev. Appl.* **3**, 014008 (2015).

[22] Diniz, I., Portolan, S., Ferreira, R., Gérard, J.M., Bertet, P. & Auffèves, A. Strongly coupling a cavity to inhomogeneous ensembles of emitters: Potential for long-lived solid-state quantum memories. *Phys. Rev. A* **84**, 063810 (2011).

[23] Houdré, R., Stanley, R.P. & Ilegems, M. Vacuum-field Rabi splitting in the presence of inhomogeneous broadening: Resolution of a homogeneous linewidth in an inhomogeneously broadened system. *Phys. Rev. A* **53**, 2711 (1996).

[24] Muñoz-Matutano, G. *et al.* Quantum-correlated photons from semiconductor cavity polaritons. arXiv:1712.05551 (2017).

[25] Ferrier, L. *et al.* Interactions in confined polariton condensates. *Phys. Rev. Lett.* **106**, 126401 (2011).

[26] Rodriguez, S.R.K. *et al.* Interaction-induced hopping phase in driven-dissipative coupled photonic micro-cavities. *Nat. Commun.* **7**, 11887 (2016).

[27] Togan, E., Lim, H.T., Faelt, S., Wegscheider, W. & Imamoğlu, A. Strong interactions between dipolar polaritons.arXiv:1804.04975 (2018).

[28] Rosenberg, I., Liran, D., Mazuz-Harpaz, Y., West, K., Pfeiffer, L. & Rapaport, R., Strongly interacting diplar-polaritons, *Sci. Adv.* **4**, eaat8880 (2018).

[29] Ravets, S. *et al.* Polaron polaritons in the integer and fractional quantum Hall regimes. *Phys. Rev. Lett.* **120**, 057401 (2018).

[30] Boulier, T. *et al.* Polariton-generated intensity squeezing in semiconductor micropillars. *Nat. Commun.* **5**, 3260 (2014).

Supplementary Information is linked to the online version of the paper at www.nature.com/nature.

Author Contributions A.D., T.F. and A.I. supervised the project. T.F. designed the experiment. A.D. and T.F. carried out the measurements. A.S., C.S., and S.H. grew the sample. A.D. and A.I. wrote the manuscript.

Author Information Reprints and permissions information is available at www.nature.com/reprints. The authors declare that they have no competing financial interests. Correspondence and requests for materials should be addressed to imamoglu@phys.ethz.ch.
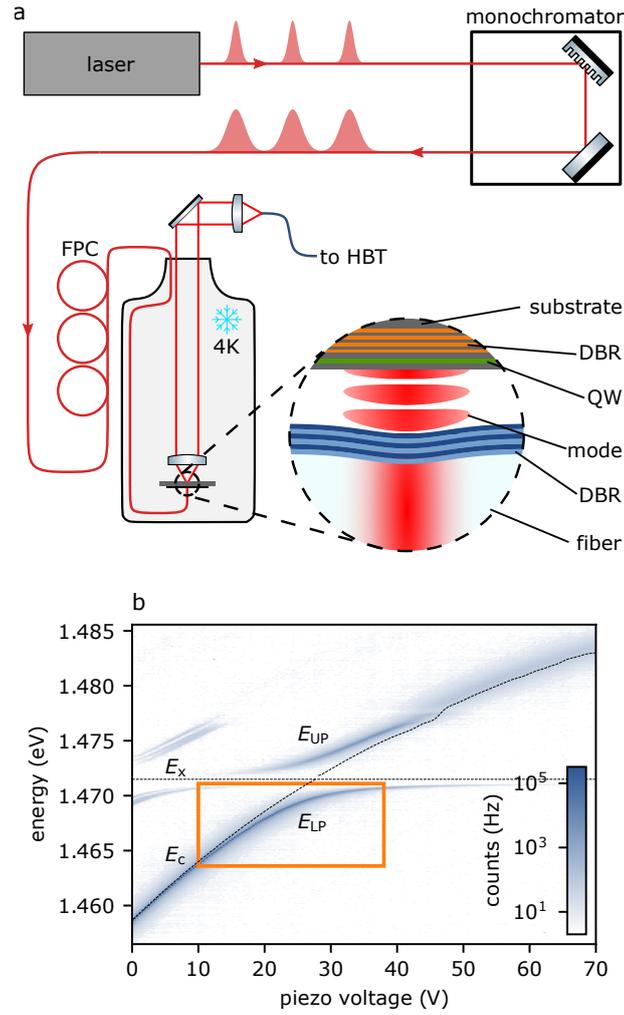
Figure 1: **Experimental set-up for cavity-polaritons.** (a) A fibre cavity is driven by either a cw laser or ps laser pulses whose pulsewidth is prolonged by a monochromator. The polarization set by fibre polarization controllers (FPC) is chosen to match the lowest linearly polarized cavity mode. The transmitted light is collected in a fibre and guided to a Hanbury Brown and Twiss (HBT) setup where photon statistics are measured. Zoom-in: Structure of the semi-integrated cavity. (b) White light transmission spectra as a function of the piezo voltage controlling the cavity length, revealing a Rabi splitting of 3.5 meV. At low piezo voltages, a transverse mode multiplet strongly coupled to the exciton is visible. Additionally, at about 1.478 eV an impurity resonance is also coupled to the cavity mode. The orange box indicates the region of interest for the present work.
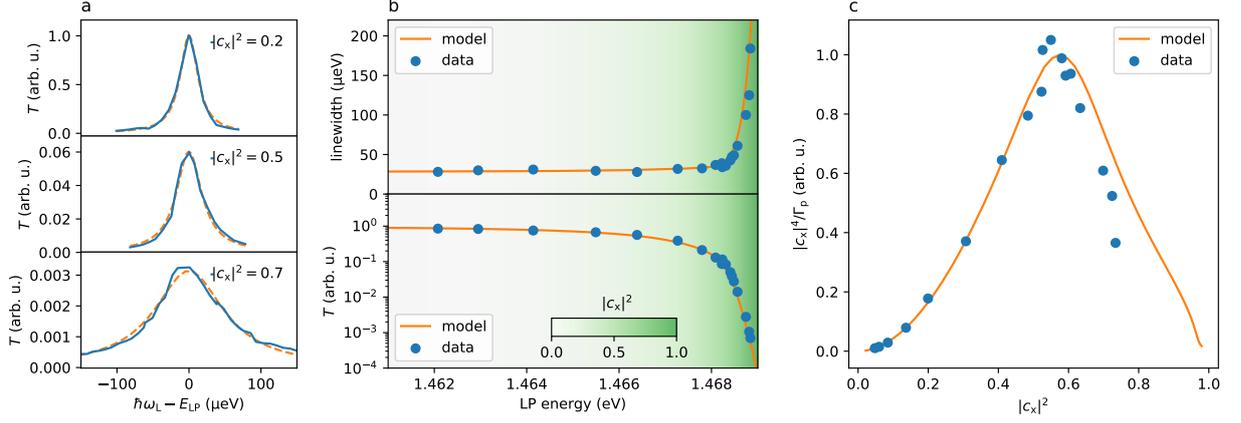
Figure 2: **Optimization of polariton parameters**. (a) Transmission spectra measured at three different cavity-exciton detunings (blue line) depicted together with the Lorentzian fit to the data (orange dashed line). (b) Upper panel: polariton linewidth Γ_p extracted from the transmission measurements, as a function of the LP energy (blue dots) and linewidth calculated from the simulation (orange curve). Lower panel: Maximum measured polariton transmission as a function of the LP energy (blue dots) and simulated maximum cavity transmission (orange curve). The background colour plot indicates the Hopfield coefficient corresponding to the lower polariton energy. (c) The ratio $|c_x|^4/\Gamma_p$ which quantifies the maximum attainable quantum correlations as a function of the exciton content $|c_x|^2$ of the lower polariton (blue dots). The calculated ratio $|c_x|^4/\Gamma_p$ (orange curve).
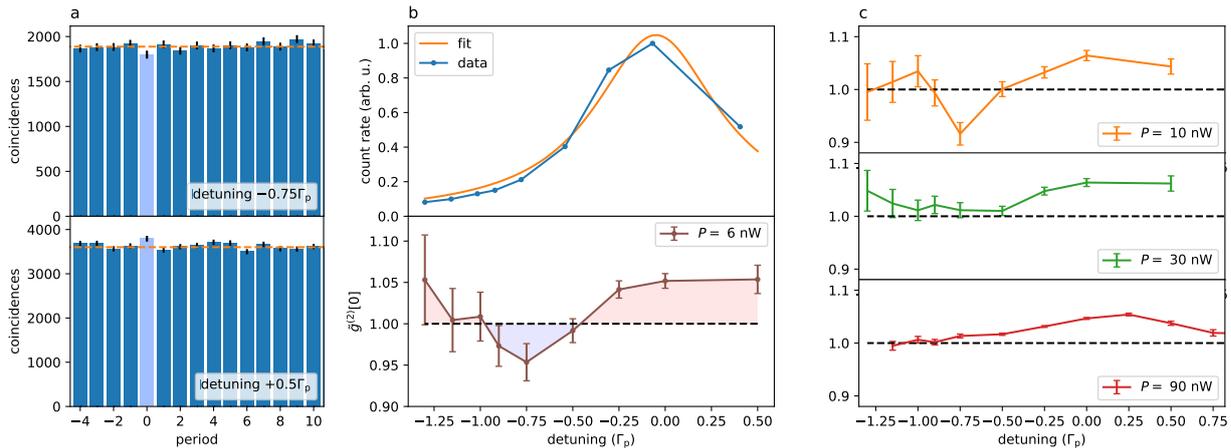
Figure 3: **Quantum correlations between polaritons.** (a) Upper panel: Coincidence number in pulsed regime as a function of the period difference between the two detected photons, at a detuning of $\Delta = -0.75\Gamma_\mathrm{p}$. The orange dashed line indicates the mean value of the non-zero periods. Lower panel: Same as the upper panel, but at a detuning of $\Delta = +0.5\Gamma_\mathrm{p}$. The error bars represent the square root of the number of coincidence events. An estimate of the standard deviation calculated from 18 uncorrelated periods gives an error bar that is in excellent agreement with the depicted values. (b) Upper panel: Photon rate as a function of the laser detuning (blue curve). Lorentzian fit to the data (orange curve). Lower panel: Integrated $\tilde{g}^2[0]$ as a function of the laser detuning. The dashed black line indicates the value for uncorrelated photons. The error bars are calculated from the Poissonian statistics of the detection events shown in (a). (c) Integrated $\tilde{g}^2[0]$ as a function of the laser detuning at higher laser powers.

METHODS

Experimental set-up. The experiments are based on an open cavity structure where the top mirror is a concave distributed Bragg reflector (DBR) mirror deposited on a fibre. A dimple with a radius of curvature of 13.9 μm is created on the centre of the fibre facet using CO_2 laser ablation. The bottom (output) mirror is integrated in the sample and consists of an AlAs/GaAs DBR grown by molecular beam epitaxy. A lambda spacer layer containing a 17 nm wide $In_{0.04}Ga_{0.96}As$ QW is grown on top of this latter DBR during the same growth process. The light transmitted through the cavity is collimated from the back of the sample and collected into a fibre that guides it to a Hanbury Brown and Twiss set-up.

Photon correlation measurements. We drive the cavity using a Ti:Sapphire picosecond laser

with 80 MHz repetition rate. We prolong the pulses using a monochromator of bandwidth 20 μeV. The centre wavelength of the laser pulses is set by controlling the grating angle. The transmitted photons are detected by two fibre-based commercial avalanche photodiodes of quantum efficiency 45 % and timing jitter 300 ps, and the detection events are recorded using a time-tagged single photon counter. The photon records are binned according to the number of laser periods ΔT separating their detection. The integrated $\tilde{g}^{(2)}[0]$ is defined as the ratio between the coincidence number with $\Delta T = 0$ to the average of the coincidence number having $\Delta T \neq 0$ calculated from 20 consecutive periods around the zero delay.

Data availability

The data that support the plots within this paper and other findings of this study are available from the corresponding author upon reasonable request.